Applied Catalysis B: Environmental 218 (2017) 60–67

Contents lists available at ScienceDirect

Applied Catalysis B: Environmental

journal homepage: www.elsevier.com/locate/apcatb

Improved photocatalytic activities of g-C_3N_4 nanosheets by effectively trapping holes with halogen-induced surface polarization and 2,4-dichlorophenol decomposition mechanism

Jiadong Li, Xuliang Zhang, Fazal Raziq, Jinshuang Wang, Chong Liu, Yanduo Liu, Jiawen Sun, Rui Yan, Binhong Qu, Chuanli Qin*, Liqiang Jing*

Key Laboratory of Functional Inorganic Materials Chemistry (Heilongjiang University), Ministry of Education, School of Chemistry and Materials Science, International Joint Research Center for Catalytic Technology, Harbin 150080, PR China

ARTICLE INFO

Article history:
Received 15 May 2017
Received in revised form 8 June 2017
Accepted 14 June 2017
Available online 16 June 2017

Keywords:
g-C_3N_4
Halogen-induced charge separation
Trapping hole
Photocatalysis
2,4-DCP degradation

ABSTRACT

It is highly desired for g-C_3N_4 nanosheets as efficient photocatalysts to greatly enhance the photogenerated charge separation by trapping holes. Herein, it is clearly demonstrated mainly by means of the steady-state surface photovoltage spectra, the time-resolved surface photovoltage responses in N_2 and the fluorescence spectra related to the produced •OH amount that the modified chloride with a proper amount could effectively trap the photogenerated holes so as to greatly enhance the charge separation of g-C_3N_4, leading to the obviously-improved photocatalytic activities for degrading 2,4-dichlorophenol (2,4-DCP) and converting CO_2 to CH_4. Interestingly, similar positive effects on g-C_3N_4 are also confirmed after modification with other halogen anions, like Br^- and F^-, whereas the Cl^- modifier is the best one. Although the used Cl^- and Br^- have different mechanism for capturing holes from the modified F^-, it is concluded that it is feasible to greatly enhance the charge separation by the halogen-induced surface polarization. As excepted, the formed •OH as the hole-modulated direct products could dominate the photocatalytic degradation of 2,4-DCP. Moreover, the possible decomposition mechanism closely related to •OH attack is proposed through the detected main intermediates. This work will help us to well understand the importance to trap the photogenerated holes for efficient photocatalysis on g-C_3N_4, and also provide a feasible strategy to improve the photocatalytic activities of g-C_3N_4 for environmental remediation and energy production.

1. Introduction

With the population growth and fossil fuel consumption, environmental and energy crises have become the primary issues to solve. For example, the chlorophenols is a group of organic pollutants which is highly stable, strong resistant to degradation [1,2]. Specially, as one of the most serious environmental hazardous pollutants, 2,4-dichlorophenol (2,4-DCP) is potentially carcinogenic and toxic which mainly arising from the wide use of pesticides, herbicides and fungicides, and it has been listed by the U.S. Environment Protection Agency as a priority control pollutant [3]. In addition, carbon dioxide (CO_2) concentration has been growing with the fossil fuel combustion [4]. It is estimated that the CO_2 content in the atmosphere rises every year with the rate higher than 2% and thus, the average temperature of the environment was increased by 0.4–0.8° C over the last century [5]. Elevated CO_2 content has led to the greenhouse effect so that the polar ice melting, sea level rising and global warming happened [6]. Thus, effective control of CO_2 emissions is essential. However, even though CO_2 is the main cause of greenhouse effect and anthropogenic, it is also a potential carbon source [7]. Therefore, the effective conversion of CO_2 to fuel is of importance, which has aroused much concern [8]. Researchers are committed to the development of thermocatalytic, electrocatalytic, and other technical methods to solve the mentioned-above environmental and energy issues. However, among various techniques, the great potential of semiconductor photocatalysis in resolving the environmental pollution and energy crisis have been noticed [9]. Since visible light is the main component of the solar spectrum, it is essential to develop visible light-driven photocatalysts. To date, enormous efforts have been devoted to exploring visible-light photocatalysts, such as Fe_2O_3, WO_3 and CdS, for pollutant degradation and CO_2 reduction [10–12].

* Corresponding authors.
E-mail addresses: chuanliqin@163.com (C. Qin), Jinglq@hlju.edu.cn (L. Jing).

http://dx.doi.org/10.1016/j.apcatb.2017.06.038
0926-3373/

In recent years, a novel polymeric graphitic carbon nitride (g-C_3N_4) has attracted tremendous attention, due to its suitable energy bandgap (2.7 eV) [13,14], high chemical stability, thermal stability and unique surface properties that are crucial in photocatalysis [15,16]. Moreover, g-C_3N_4 exhibits an appropriate microstructure with unsaturated nitrogen atoms for anchoring active sites [17]. Due to these superior properties, g-C_3N_4 has been proven to have promising applications in environmental and sustainable energy fields as heterogeneous metal-free photocatalysts for pollutant degradation and CO_2 reduction under solar irradiation [18,19]. However, its photocatalytic performance under solar light irradiation is still not satisfactory. This is generally attributed to small specific surface area, limited visible-light absorption and weak charge separation. For this, the photocatalytic activity is greatly improved by compounding fish-scale structured g-C_3N_4 nanosheet to increase the surface area [20]. It is also an effective method to improve the photocatalytic activity by non-metals doping such as B, C, O, S and P, to extend the visible-light response [21–24]. There are feasible ways to enhance the separation of photogenerated charges by constructing heterojunctions with other semiconductors. For example, graphene quantum dots modified g-C_3N_4, leading to the obviously-improved photocatalytic activities [25]. However, among various modification methods, its low valence band bottom position (1.4 eV) is often ignored. This indicates that the photogenerated holes of g-C_3N_4 do not possess enough energy to induce the oxidation reaction with H_2O thermodynamically. Therefore, it is much feasible to modulate holes for efficient photocatalysis of g-C_3N_4.

As for the photogenerated holes with low energy, it has been successfully developed to construct a Z-schemed nanocomposite by coupling a narrow band-gap oxide, in which g-C_3N_4 and the coupled oxide are excited simultaneously. The photogenerated electrons of used oxide are transferred to the valence band of g-C_3N_4, and then recombine with the photogenerated holes in g-C_3N_4 [26,27]. Hence, the photogenerated electrons in g-C_3N_4 and the photogenerated holes in the used oxide could exhibit strong reduction and oxidization ability, respectively. This could lead to the enhanced charge separation and hence the improved photocatalytic activity. But in this case, it needs two photons for an effective photocatalytic reaction so that it has limited photoactivity improvement. Hence, it is desired to develop another effective way to regulate the photogenerated holes. Since the holes are positively charged, it is naturally expected that it is an effective way to modulate holes by creating surface polarization, including the formed surface negative field and the modified strong-negativity anions. In our previous works, it has been demonstrated that the formed negative field after phosphate modification could promote the separation of photogenerated carriers on $BiVO_4$ and TiO_2 [28], leading to the greatly-improved photoactivities. It has been revealed that modified chlorides on the surfaces of TiO_2 could trap photogenerated holes so as to enhance the charge separation and to improve the photoactivity for CO_2 reduction [29]. Thus, it is expected that it is possible to improve the photocatalytic activities of g-C_3N_4 for pollutant degradation and CO_2 conversion by modifying chlorides to effectively trap holes. Moreover, it is also possible to use other halogen ions like F^- and Br^- to modify g-C_3N_4. To the best of our knowledge, similar modification on g-C_3N_4 has seldom been reported up to now. Therefore, it is much meaningful to carry out the modification with halogen ions to improve the photocatalytic activities and to reveal the mechanism.

As commonly known, hydroxyl radicals (•OH) could be produced by the reactions of photogenerated holes with H_2O, further attacking organic pollutants in the degradation of organic pollutants and evolving O_2 in the reduction of CO_2. Obviously, •OH plays an important role in photocatalysis. Therefore, it has great significance to investigate the produced •OH in details for deeply revealing the charge separation and related mechanism. In addition, the photocatalytic degradation mechanism of 2,4-DCP as a typical pollutant is ambiguous [30,31]. In different systems, it may be attacked by holes (h^+), superoxide radicals ($^{\bullet}O_2^-$) or •OH, subsequently inducing the dechlorination and open-loop degradation [32]. And also, it has been seldom explored in the photocatalysis on the bases of g-C_3N_4, especially for the hole-modulated g-C_3N_4. Hence, it is very meaningful to clarify the above fact on the photocatalytic decomposition mechanism of 2,4-DCP on g-C_3N_4.

Based on the above discussion, we have investigated the effects of modification with halogen ions on the photocatalytic activities of g-C_3N_4. It is demonstrated that the modification with halogen ions could greatly improve the photoactivities for 2,4-DCP degradation and CO_2 reduction, especially for the modified Cl^-. This is attributed to the enhanced charge separation by effectively modulating the photogenerated holes. It is confirmed that the modified Cl^- and Br^- have different mechanism for trapping holes from the modified F^-. Moreover, the dominant radical species to firstly attack the 2,4-DCP is explored on modified g-C_3N_4, along with the detailed decomposition paths of 2,4-DCP. This work would provide us with a much feasible route to improve the photocatalytic activities of g-C_3N_4-based photocatalysts by modulating the photogenerated holes to purify polluted environments and to convert CO_2 into fuels.

2. Experimental

All the chemicals were of analytic grade and used as-received without further purification. Deionized water was used throughout the reaction.

2.1. Materials synthesis

2.1.1. Synthesis of g-C_3N_4 (CN)

CN was synthesized by heating urea in semi-cover ceramic crucible at 550 °C for 3 h with the rate of 0.5 °C/min. After that, the ceramic crucible was cooled to room temperature naturally. The obtained light yellow product was grinded into fine powder for further experimental work.

2.1.2. Chloride-modified CN (Cl/CN)

CN was successfully modified with chloride, by mixing of as prepared CN and different amounts of hydrochloric acid. In a typical procedure, 1 g of CN powders was dispersed into 30 mL of planned-concentration hydrochloric acid solution by vigorously stirring for 1 h. Subsequently, the suspension was dried at 80° C and then calcined at 400° C for 1 h. The hydrochloric acid modified samples are denoted as XCl/CN, in which CN is g-C_3N_4 and X means the molar ratio percentage of used HCl to CN.

2.1.3. Other halide anion (F^- and Br^-) modified CN

The methods of fluoride-modified (F/CN) and bromide-modified (Br/CN) g-$C_3N_4$are the same as the above-mentioned chloride modification. 1 g of CN powders was dispersed into 30 mL of planned-concentration hydrofluoric acid or hydrobromic acid solution by vigorously stirring for 1 h. Subsequently, the suspension was dried at 80 ° C and then calcined at 400 ° C for 1 h.

2.2. Characterization techniques

The samples were analyzed by various methods. The X-ray diffraction (XRD) was tested with a Rigaku D/MAX-rA powder diffractometer, using Cu Kα radiation. UV–vis diffuse reflectance spectra (DRS) were recorded with a Model Shimadzu UV-2550 spectrophotometer, using $BaSO_4$ as reference. The photoluminescence (PL) spectra of the samples were measured with a

spectrofluoro-photometer (LS55Perkin-Elmer) at excitation wavelength of 390 nm. The X-ray photoelectron spectroscopy (XPS) was examined by using a Model VG ESCALAB apparatus with Mg K Xray source, and the binding energies were calibrated with respect to the signal for adventitious carbon (binding energy = 284.6 eV). The steady-state surface photovoltage spectroscopy (SS-SPS) measurements of the samples were carried out with a home-built apparatus. The powder sample was sandwiched between two ITO glass electrodes, which were arranged in an atmosphere-controlled sealed container. The SS-SPS signals were the potential barrier change of the testing electrode surface between that in the presence of light and that in the dark. The signal was collected by a lock-in amplier (SR830) synchronized with a light chopper (SR540). The mono-chromatic light was obtained by passing light from a 500W Xenon lamp (CHF XQ500W) through a double prism monochromator (SBP300).

Time-resolved surface photovoltage (TR-SPV) measurements of samples were operated by the process in which the sample chamber connected an ITO glass as top electrode and a steel substrate as bottom electrode, and a mica spacer of 10 μm thick was placed between the ITO glass and the sample to decrease the space charge region at the ITO-sample interface. The samples were excited by a radiation pulse of 355 nm with 10 ns width from a second harmonic Nd: YAG laser (Lab-130-10H, Newport, Co.). Intensity of the pulse was measured by a high energy pyroelectric sensor (PE50BF-DIF-C, Ophir Photonics Group). The signals were amplified with a preamplier and then registered by a 1 GHz digital phosphor oscilloscope (DPO 4104B, Tektronix). The TR-SPV measurements were performed in N_2 atmosphere at room temperature.

2.3. Analysis of hydroxyl radical

0.02 g of samples was dispersed in 60 mL coumarin aqueous solution (0.001 M) in a beaker. Prior to irradiation, the reactor was magnetically stirred for 10 min to attain an adsorption-desorption equilibrium. After irradiation for 1 h with a 150 W Xenon lamp (GYZ220 made in China), the sample was centrifuged, and then a certain volume of solution was transferred into a Pyrex glass cell for the fluorescence measurement of 7-hydroxycoumarin at 332 nm excitation wavelength with an emission peak wavelength at 460 nm through the above-mentioned spectrofluorometer.

2.4. Evaluation of photoactivities

2.4.1. Photocatalytic experiments for degrading organic pollutants

The photocatalytic activities of the samples were tested by degrading 2,4-DCP and phenol under light irradiation, respectively. A 150 W Xenon lamp was chosen as a light source. In a typical liquid-phase photocatalytic degradation experiment, 0.15 g of photocatalyst and 60 mL of 10 mg/L 2,4-DCP or phenol aqueous solution were mixed by stirring in dark for 30 min to reach the adsorption-desorption equilibrium. Then, the photocatalytic reaction was carried out for 30 min in an open glass reactor. The distance between the light source and the reactor was 10 cm. After centrifugation, the 2,4-DCP concentrations were analyzed at the characteristic optical adsorption (285 nm) of 2,4-DCP with a Shimadzu UV-2550 spectrophotometer and the phenol concentrations were analyzed by 4-aminoantipyrine spectrophotometric method at the characteristic optical adsorption (510 nm) of phenol. In addition, for the photocatalytic degradation of rhodamine B (RhB), 0.2 g of photocatalyst and 100 mL of 15 mg/L RhB solution were used, and the experiments were performed in a similar way to the photocatalytic degradation of 2,4-DCP.

2.4.2. Photocatalytic experiments for CO_2 conversion

0.2 g of samples was dispersed in 10 mL deionized water contained in a cylindrical steel reactor with 100 mL volume and 3.5 cm^2 area. A 300 W Xenon arc lamp was used as the light source. High pure CO_2 gas was passed through water and then entered into the reaction setup for reaching ambient pressure. The used photocatalyst was allowed to equilibrate in the CO_2/H_2O system for 30 min. During irradiation, about 0.5 mL of gas production was taken from the reaction cell at given time interval for subsequent CH_4 concentration analysis by using a gas chromatograph (GC-2014 with FID detector, Shimadzu Corp, Japan)

2.5. Measurements of produced intermediates

The intermediates were detected during the photocatalytic degradation of 2,4-DCP. In a typical experiment, 0.15 g Cl/CN was mixed with 80 mL of 10 mg/L 2,4-DCP solution by a magnetic stirrer for 0.5 h in the dark to maintain the adsorption desorption equilibrium of the reaction system. After that, the system began to be irradiated with 150 W Xenon lamp for 4 h. At the interval of every 1 h, a planned amount of the solution was centrifuged and the concentration of 2,4-DCP was analyzed by UV spectrometer. The intermediates were analyzed with Agilent liquid chromatography tandem mass spectrometry (LC/MS, 6410MS, USA) technique. The intermediate fragments of the main reaction were analyzed through scan mode.

3. Results and discussion

3.1. Structural characterization and surface composition

The crystal composition and structure of the synthesized samples were analyzed by XRD patterns. Fig.S1A shows the XRD patterns of CN with different ratios of modified chloride. Two characteristic diffraction peaks of CN are found, which are indexed to $2\theta = 27.3^\circ$ (002) and $2\theta = 13.1^\circ$(100), respectively [33]. It is shown that the crystal structure of CN does not change after chloride modification. It is evaluated from the DRS spectra (Fig.S1B) that the optical absorption range of CN is not changed after chloride modification. The band gap energy is about 2.7 eV, which is calculated by a widely accepted equation, $E_g = 1240/\lambda$ [34,35]. The TEM micrographs of CN and 7Cl/CN samples are shown in Fig. S2A and 2B, respectively. The CN shows a slice-like morphology, and its morphology has no change after chloride modification. Therefore, it can be concluded that the chloride modification does not change the crystal phase composition, optical absorption and morphology of CN.

To further validate the presence of chlorine, the XPS spectra of CN and 7Cl/CN is shown in Fig.S3. The main N1 s peak at 398.6 eV is attributed to sp^2-hybridized nitrogen (C═N—C). The weak characteristic peaks at 399.8 and 401.5 eV are assigned to the bond energies of N in N—$(C)_3$ and C—N—H, respectively (Fig.S3A). As for pure CN, the characteristic peak of C1s is centered at 288.3 eV and 284.6 eV, attributed to the C—N—C band and C═C band, respectively (Fig. S3B) [36]. As shown in Fig. S3C, the characteristic peak of Cl2p on modified CN at 197.3 eV is confirmed. It is found that the position of C1s characteristic peak changes after chloride modification, indicating that Cl replace the hydroxyl group on the surface and connected with C atom in the modified sample [37]. Based on the XPS results, it is deduced that the chloride is successfully modified on the surface of resulting CN.

3.2. Photophysical and photochemical properties

The steady-state surface photovoltage spectra (SS-SPS) and time-resolved surface photovoltage (TR-SPV) responses are direct

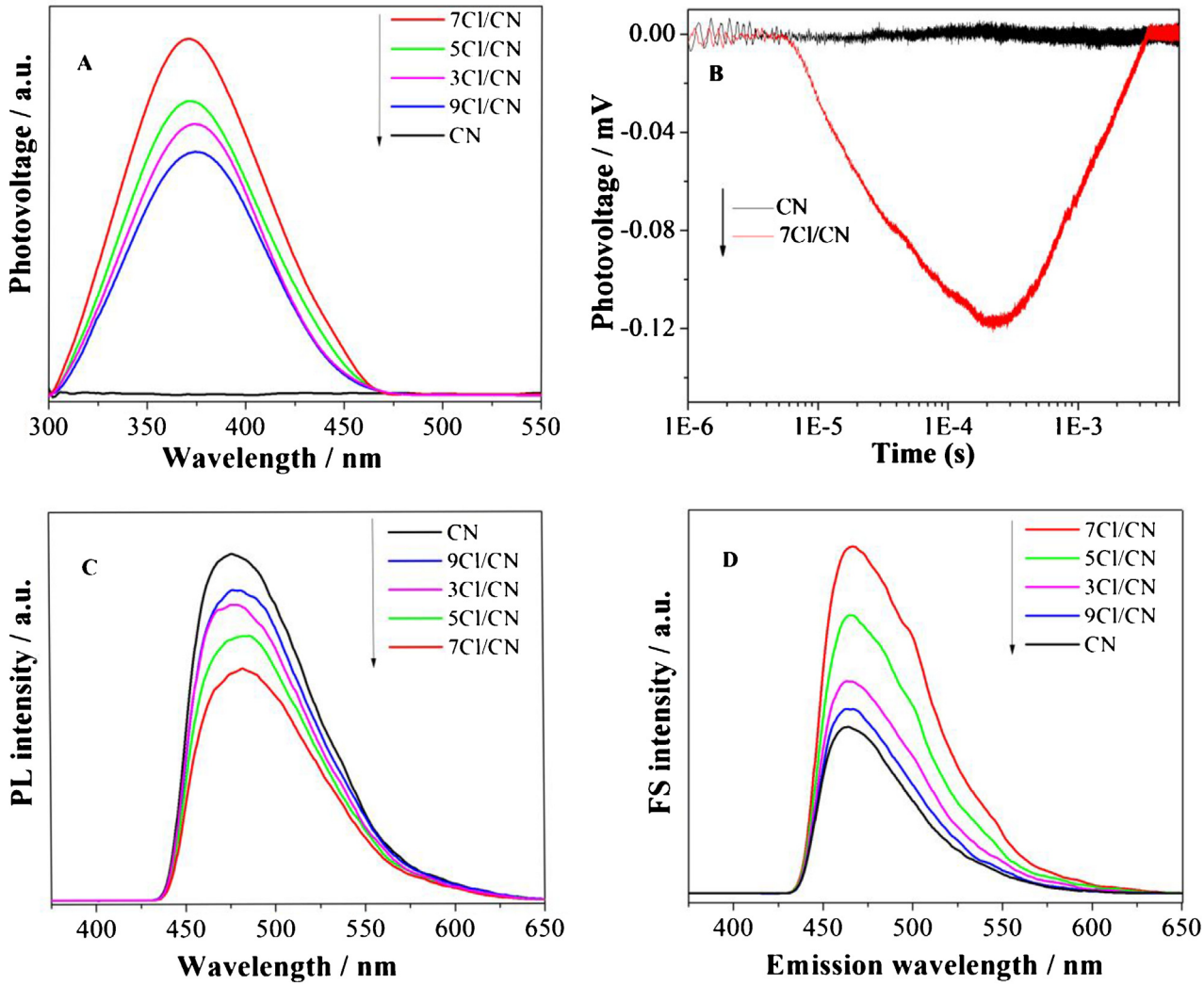

Fig. 1. SS-SPS (A) and TR-SPV (B) responses in nitrogen, PL spectra (C) and FS spectra related to the amount of produced •OH (D) of CN and XCl/CN samples, in which CN means pure g-C_3N_4, Cl/CN is chloride-modified g-C_3N_4, and X is the molar percentage of used Cl to CN. It is the same unless stated elsewhere.

and reliable means to investigate the nature of photogenerated charges in solid-state semiconductors. The intensity of the SS-SPS signal reflects the separation of the photogenerated electron-hole pairs, and the TR-SPV signal reflects the lifetime of the photogenerated carriers in the semiconductor material. In general, the stronger is the SPS response, the higher is the photogenerated charge separation. The SS-SPS responses of CN and XCl/CN in N_2 are shown in Fig. 1A. It is clear that pure CN has no SPS signal, while it is apparent that the SS-SPS response of CN is significantly enhanced after modification with a certain amount of chloride, indicating the enhanced charge separation and it is the strongest response for 7Cl/CN. However, the SS-SPS response begins to decrease if the amount of modified chloride is continuously increased. Moreover, the TR-SPV responses of CN and 7Cl/CN are investigated in N_2 atmosphere as shown in Fig. 1B. One can notice that there is no TR-SPV response for CN, indicating a high charge recombination. However, the chloride-modified CN exhibits a negative TR-SPV signal. This is because that the used chloride could effectively trap holes so as to make the corresponding electrons preferentially diffuse to the surfaces of tested electrode in N_2. Interestingly, it can be seen that the carrier lifetime of CN after modifying chloride is prolonged by several milliseconds. This further proves that the chloride modification is favorable for the charge separation enhancement.

The photoluminescence (PL) spectra were recorded to further investigate the photogenerated charge properties of CN and XCl/CN as shown in Fig. 1C. One can see that CN exhibits a strong signal centering at 470 nm, and the energy of this PL signal is closely related with optical band-gap energy of CN (2.7 eV). Noticeably, the PL intensity of CN is significantly decreased after modifying a proper amount of chloride, and the 7Cl/CN exhibits the lowest PL response, indicating the lowest recombination of electron-hole pairs. It is consistent with the above SS-SPS results.

It is proved by the above photo-physical properties that the charge separation of g-C_3N_4 is enhanced after chloride modification. Is it possible to support the enhanced charge separation by the crucial photochemical radical product, •OH? For this, the fluorescence spectra (FS) related to the produced •OH amount are shown in Fig. 1D. It is clearly seen that pure CN produces a small amount of •OH, while the amount of •OH generated is increased after chloride modification. As expected, the optimized 7Cl/CN shows the strongest FS intensity, corresponding to the highest charge separation. Obviously, it is in good agreement with the above SS-SPS and PL results. Therefore, it could be concluded that the photogenerated charge separation ofg-C_3N_4 is enhanced by modifying a proper amount of chloride.

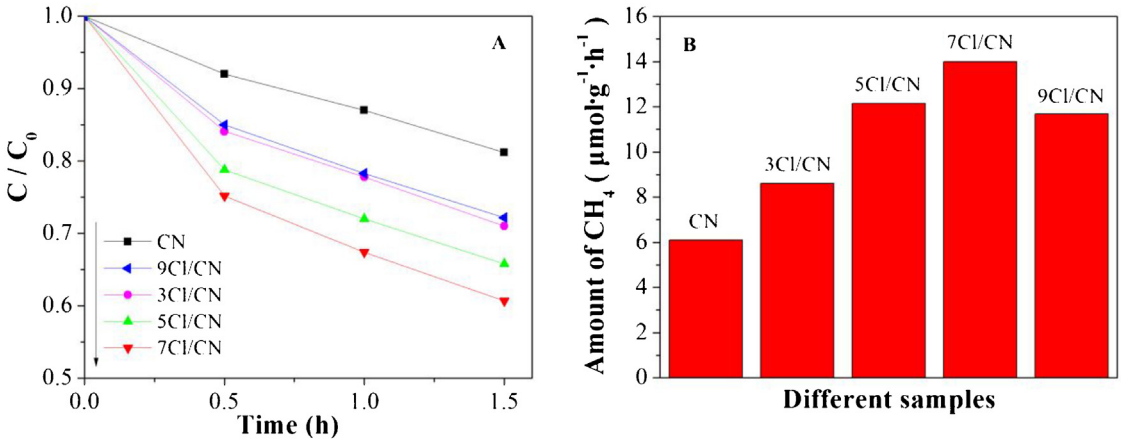

Fig. 2. Photoactivities for 2,4-DCP degradation(A) and CO_2 reduction(B) of CN and XCl/CN.

3.3. Photocatalytic activities for pollutant degradation and CO_2 reduction

The photocatalytic activities of CN and XCl/CN were investigated for 2,4-DCP degradation, as shown in Fig. 2A. It is clearly seen that pure g-C_3N_4 exhibits poor photocatalytic activity for 2,4-DCPdegradation, and the photoactivity could be enhanced after chloride modification. In particular, 7Cl/CN exhibits the highest photocatalytic activity. As the amount of used chloride continues to increase, the activity of photocatalytic degradation of 2,4-DCP begins to decrease.

To further support this result, we have measured the degradation of phenol and RhB (Fig. S4A), it is clearly found that 7Cl/CN exhibits the best photocatalytic performance. Compared to pure CN, the degradation rate of 7Cl/CN is improved by 4.1 and 2.3 times respectively in the degradation of phenol and RhB. If the amount of chloride is too much, the photocatalytic activities begin to decrease. It is well consistent with the above result. The stability of 7Cl/CN was also measured, as shown in Fig. S4B. It shows that the degradation rate of the 7Cl/CN is nearly not changed after four cycles, indicating that the chloride-modified CN is stable.

As shown in Fig. 2B, the photocatalytic results for CO_2 reduction in water system without any cocatalyst are demonstrated for CN and XCl/CN. One can see that pure CN exhibits poor activity for CO_2 conversion to CH_4 as the detected main gas-phase product, and the CH_4 production rate is 6.1 $\mu mol\, g^{-1}\, h^{-1}$. With the increase in the amount of modified Cl^-, the rate of CH_4 production gradually increases. Noticeably, 7Cl/CN exhibits the best performance, and its rate of CO_2 conversion to CH_4 is 14 $\mu mol\, g^{-1}\, h^{-1}$ by 2.3-time enhancement compared to pure CN. In addition, it is found from Fig. S4C that the optimized 7Cl/CN produces a larger amount of O_2 than pure CN, further indicating its high activity. Obviously, the photocatalytic activity results are consistent with the ones of SS-SPS responses. Therefore, it is concluded that the improved photocatalytic activity is mainly attributed to the enhanced photogenerated charge separation caused by the modification of chloride.

3.4. Effects of different halide anion modification

Since the modified chloride ions on the surface of g-C_3N_4 could capture holes so as to promote the charge separation and hence to improve the photocatalytic activity. To verify the effects of other halogen anion modification on g-C_3N_4, we have also completed its modification with two other halide anions, like fluoride and bromide, with the same amount as that of the optimized chloride (7%). The structural characterization is shown in Fig. S5. As shown, there is no new XRD peak after fluoride ions (F^-) or bromide ions (Br^-) modification. It can be seen from DRS spectra (Fig. S5B) that the optical absorption of g-C_3N_4 modified by F^- or Br^- has not changed. Hence, it is concluded that the modification of g-C_3N_4 by F^- or Br^- does not change the crystal phase composition and optical absorption. To investigate whether fluoride or bromide are modified on the surfaces of g-C_3N_4, XPS measurements of 7F/CN and 7Br/CN samples were performed, as shown in Fig.S5C and 5D. The peak at 684.1 eV is observed (Fig. S5C), corresponding to F1s characteristic peak, and the peak at 68.4 eV is regarded as the characteristic peak of Br3d (Fig. S5D) [38,39]. According to the XPS results, it is confirmed that the fluoride and the bromide ions are modified on the surfaces of g-C_3N_4.

To investigate the photocatalytic activity of CN modified with different halide, photocatalytic experiments for degrading 2,4-DCPhave been carried out. As shown in Fig. 3A, the degradation rates of halide-modified CN are obviously higher than that of pure CN. And the 7Cl/CN shows the highest degradation activity, and its degradation rate is 2.8-time higher than that of pure CN. The degradation activity of 7Br/CN is higher than that of 7F/CN. For further comparison, we have also conducted the CO_2 reduction test. Fig. 3B shows the kinetic curves of photocatalytic reduction of CO_2 on different halide-modified CN samples. It can be seen that the photocatalytic activity for CO_2 conversion of the halogen-modified CN samples are significantly better than that of pure CN. The activity of 7Cl/CN is the highest. Noticeably, the conversion rate of CO_2 to CH_4 of 7Br/CN is higher than that of 7F/CN. It is consistent with the rule of degradation of 2,4-DCP. Hence, it can be concluded that the photocatalytic activities of CN could be improved obviously by modifying halogen ions, and the activity of chloride modified sample is the best.

Compared to pure CN, the halogen-modified CN samples exhibit high FS signal related to the formed $^{\bullet}OH$ amount (Fig. 3C), and it is the strongest FS signal for 7Cl/CN, and 7Br/CN shows higher FS signal than 7F/CN. Thus, it is confirmed that the halide anion modification could promote charge separation, which is responsible for the above-tested photocatalytic activities. To explore the enhanced charge separation mechanism after halide modification, we measured the SS-SPS response of different halogen-modified samples, including 7F/CN/,7Cl/CN and 7Br/CN inN_2 atmospheres, as shown in Fig. 3D. Interestingly, 7Cl/CN and 7Br/CN exhibit significant SPS responses in N_2, and the SS-SPS response of 7Cl/CN is higher than 7Br/CN. However, 7F/CN has no SS-SPS signal. This indicates that the modified Cl^- and Br^- would have different mechanism for capturing holes from the modified F^-. This is because that it is much difficult for F^- to capture positive holes and then to be oxidized compared with Cl^- and Br^- because of the too strong electronega-

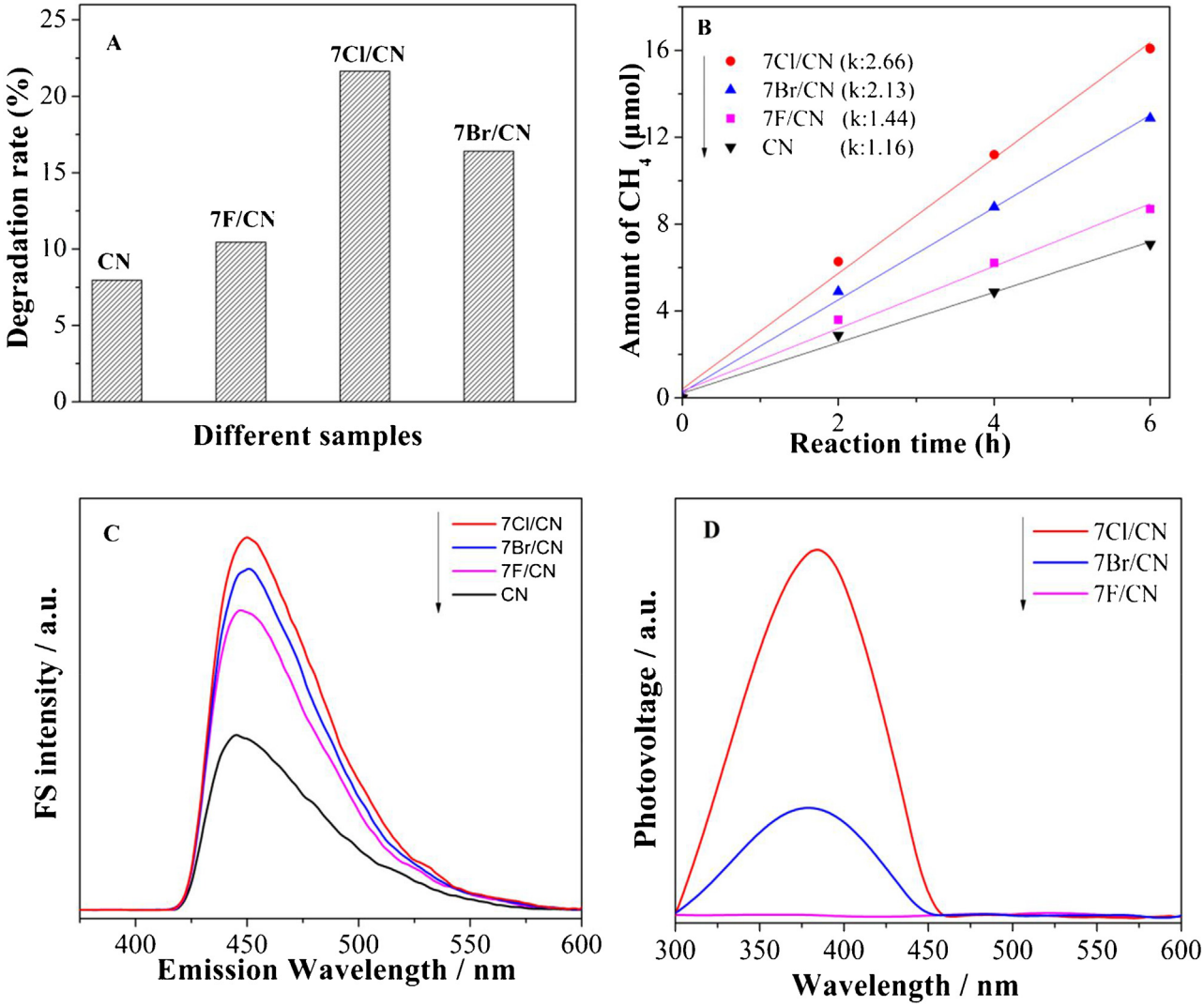

Fig. 3. Photocatalytic activities for 2,4-DCP degradation (A) and CO_2 reduction (B), FS spectra related to the amount of produced •OH (C) and SS-SPS responses in nitrogen (D) of different halogen-modified CN.

tivity of F^-. However, it could form a negative electronic field as the surface polarization after fluoride modification, which would trap the photogenerated holes so as to promote the charge separation. It is worthy of noting that the modification with halogen ions could capture/trap holes, leading to the enhanced charge separation and hence to the improved photoactivities.

3.5. Degradation pathway

In general, superoxide radicals ($•O_2^-$), active holes (h^+) or hydroxyl radicals (•OH) participate in the reaction as the main attacking species during the photocatalytic degradation of organic pollutants. In order to further investigate the mechanism of degradation of 2,4-DCP, ethylenediamine tetraacetic acid disodium salt (EDTA-2Na), benzoquinone (BQ) and isopropanol (IPA) are used as scavengers to study the effect of h^+, $•O_2^-$ and •OH in the reaction [40]. A series of experiments were carried out to examine the effects of different reactive species on the photodegradation rate of 2,4-DCP. As shown in Fig. 4A, with 1 mM of EDTA-2Na or IPA added to the system of pure CN, there is no significant change in degradation rate of 2,4-DCP. However, 1 mM BQ added to the reaction system results in a significant decrease in degradation rate compared to absence of any scavenger degradation. Therefore, it can be deduced that $•O_2^-$ is the vital species in the degradation of 2,4-DCP for pure CN. However, we have surprisingly found that when 1 mM IPA is added into the reaction system of 7Cl/CN, the degradation rate of 2,4-DCP decreased significantly as given in Fig. 4B. While the addition of BQ or EDTA-2Na in the reaction system has no change distinctly. It shows that •OH is the crucial offensive species in the process of degrading 2,4-DCP for 7Cl/CN.

To further explain the degradation mechanism, the intermediates during the degradation of 2,4-DCP by 7Cl/CN photocatalyst were analyzed by liquid chromatography tandem mass spectrometry. All the mass spectra of the intermediates are shown in Fig. S6A-F. According to the monitored intermediates, we hypothesized that a reasonable pathway for the degradation of 2,4-DCP by 7Cl/CN photocatalyst in Scheme 1. It is obviously that •OH would directly attack the aromatic ring to remove single Cl^- as the first key step to form 2-chloro-hydroquinone (m/z = 143.5).

The 143.5 signal is further supported by the LC–MS/MS with Product Ion mode as the insert in Fig. S6A. It is deduced that the observed 1,4-benzoquinone (m/z = 107.1) resulted from the fragments of 2-chloro-hydroquinone (m/z = 143.5). In the second step, the produced •OH attacks on the aromatic ring to produce 2-chloro-5-hydroxyoyclohexa-benzoquinone (m/z = 157.5 as shown Fig. S6B). We speculate this structural formula pass by the

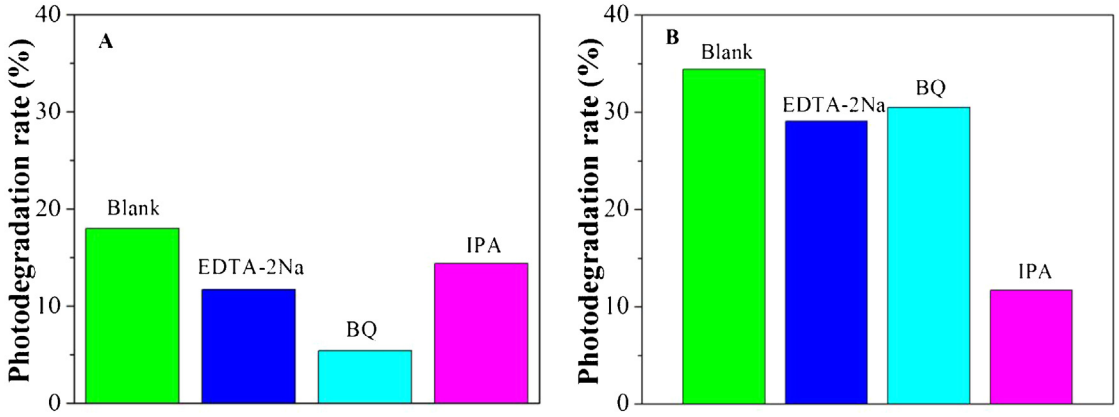

Fig. 4. Photocatalytic degradation rates of 2,4-DCP in the presence of IPA, BQ and EDTA-2Na after irradiation for 1 h on CN (A) and 7Cl/CN (B) photocatalysts.

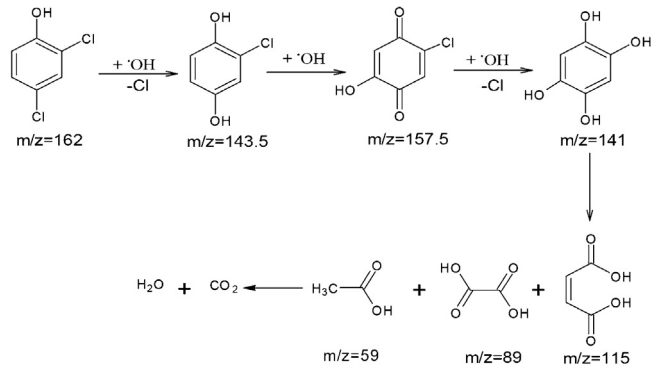

Scheme 1. Proposed pathway for 2,4-DCP degradation on 7Cl/CN photocatalyst.

LC–MS/MS with Product Ion mode as the insert in Fig. S6B. It can be inferred that 2-hydroxy-1.4-benzoquinone (m/z = 125) is an important fragment of 157.5. In the process of removing the second Cl^-, •OH would directly attack and produce 1,2,4,5-benzenetriol according to the detected m/z value of 141 (Fig. S6C). It is clear that the peak with m/z = 157.5 is obviously increased with the increase in irradiation time from 1 h to 2.5 h (Fig. S7), suggesting that the 2-chloro-5-hydroxy-1,4-benzoquinone is a little difficult to be degraded to 1,2,4,5-benzenetriol (m/z = 141), with the help of •OH. Therefore, it can be confirmed that •OH attack to remove the second Cl is very difficult in the process of degradation of 2,4-DCP. As shown in Fig. S6D-F, the target product continues ring-opening cleavage, to generate maleic acid (m/z = 115), oxalic acid (m/z = 89) and acetic acid (m/z = 59). Along with the beginning step for removing first Cl by •OH, it is understandable that the •OH should play an important role in the degradation 2,4-DCP, and it is much difficult to remove the second Cl before the aromatic ring opening.

3.6. Discussion on mechanism

In order to further understand the photocatalytic activity-improved mechanism of g-C_3N_4 after halogen ions modification, a mechanism schematic is proposed, as shown in Fig. 5. After a proper amount of halogen anion is modified on the surfaces of g-C_3N_4, the photogenerated holes could be effectively captured, further leading to the enhanced charge separation. As a result, the photocatalytic activities are markedly improved for degrading 2,4-DCP, phenol, RhB and converting CO_2 to CH_4. Among the modified three kinds of halogen anions, the modified Cl^- is the best modifier to improve the photoactivity of g-C_3N_4. It is worthy of noting that it is much beneficial for •OH formation to modify halogen anions on the surfaces of g-C_3N_4 by capturing holes. Thus, the O_2 evolution as the oxidation

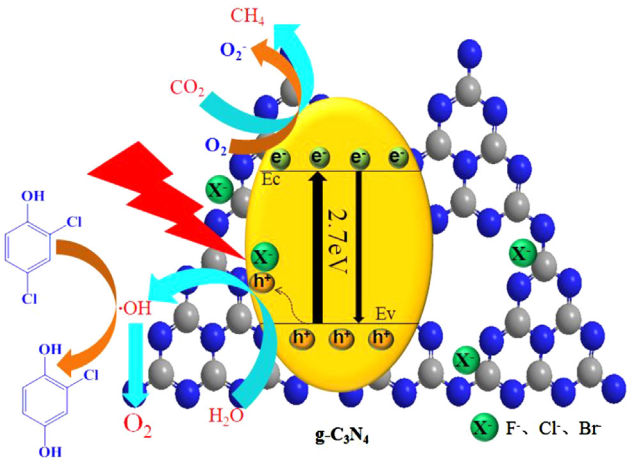

Fig. 5. Process mechanism schematic of transfer and separation of photogenerated charges, along with their induced initial photochemical reactions on the halogen-modified g-C_3N_4.

product is favored during the process of CO_2 conversion, while it is much favorable to induce the degradation of organic pollutants. In particular, it is confirmed that the formed •OH would effectively attack 2,4-DCP to initiate the degradation on Cl^- modified g-C_3N_4.

4. Conclusions

In summary, the modification with halogen anion could greatly enhance the photogenerated charge separation of g-C_3N_4 by effectively capturing hole. This is well responsible for the obviously-improved photocatalytic activities for degrading organic pollutants and converting CO_2 to CH_4. In particular, the modified Cl^- is the best to enhance the charge separation and hence to obviously improve the photocatalytic activity of g-C_3N_4. It is confirmed that the modified Cl^- and Br^- could directly capture the holes, while the modified F^- is to capture the holes by forming the negative field on the g-C_3N_4 surfaces. It is concluded that it is feasible to greatly enhance the charge separation by the halogen-induced surface polarization. Moreover, the formed •OH as the hole-modulated direct products could dominate the photocatalytic degradation of 2,4-DCP for Cl/CN. Furthermore, the possible decomposition mechanism close related to •OH attack is proposed. This work will help us to well understand the importance to capture the photogenerated holes for efficient photocatalysis on g-C_3N_4, and also provide a feasible strategy to improve the photocatalytic activities of g-C_3N_4 for environmental remediation and energy production.

Acknowledgements

We are grateful for financial support from the NSFC (U1401245 and 91622119), the Program for Innovative Research Team in Chinese Universities (IRT1237), the Project of Chinese Ministry of Education (213011A) and the Science Foundation for Excellent Youth of Harbin City of China (2014RFYXJ002).

Appendix A. Supplementary data

Supplementary data associated with this article can be found, in the online version, at **http://dx.doi.org/10.1016/j.apcatb.2017.06.038**.

References

[1] M. Pera-Titus, V. Garcıía-Molina, M.A. Baños, J. Giménez, S. Esplugas, Appl. Catal. B Environ. 47 (2004) 219–256.
[2] Y. Hou, X. Li, X. Zou, X. Quan, G. Chen, Environ. Sci. Technol. 43 (2009) 858–863.
[3] M. Humayun, Y. Qu, F. Raziq, R. Yan, Z. Li, X. Zhang, L. Jing, Environ. Sci. Technol. 50 (2016) 13600–13610.
[4] J. Ettedgui, Y. Diskin-Posner, L. Weiner, R. Neumann, J. Am. Chem. Soc. 133 (2011) 188–190.
[5] G. Sneddon, A. Greenaway, H.H.P. Yiu, Adv. Energy Mater. 4 (2014) 1301873.
[6] E.S. Sanz-Pérez, C.R. Murdock, S.A. Didas, C.W. Jones, Chem . Rev. 116 (2016) 11840–11876.
[7] S. Sen, D. Liu, G.T.R. Palmore, ACS Catal. 4 (2014) 3091–3095.
[8] H. Shi, G. Chen, C. Zhang, Z. Zou, ACS Catal. 4 (2014) 3637–3643.
[9] M.R. Hoffmann, S.T. Martin, W. Choi, D.W. Bahnemann, Chem. Rev. 95 (1995) 69–96.
[10] G.K. Pradhan, D.K. Padhi, K.M. Parida, ACS Appl. Mater. Interfaces 5 (2013) 9101–9110.
[11] X. Chen, Y. Zhou, Q. Liu, Z. Li, J. Liu, Z. Zou, ACS Appl. Mater. Interfaces 4 (2012) 3372–3377.
[12] J. Jin, J. Yu, D. Guo, C. Cui, W. Ho, Small 11 (2015) 5262–5271.
[13] F. He, G. Chen, Y. Yu, S. Hao, Y. Zhou, Y. Zheng, ACS Appl. Mater. Interfaces 6 (2014) 7171–7179.
[14] X. Zhang, X. Xie, H. Wang, J. Zhang, B. Pan, Y. Xie, J. Am. Chem. Soc. 135 (2013) 18–21.
[15] G. Liu, P. Niu, C. Sun, S.C. Smith, Z. Chen, G.Q. Lu, H.-M. Cheng, J. Am. Chem. Soc. 132 (2010) 11642–11648.
[16] J. Tian, Q. Liu, A.M. Asiri, A.O. Al-Youbi, X. Sun, Anal.Chem. 85 (2013) 5595–5599.
[17] G. Dong, L. Yang, F. Wang, L. Zang, C. Wang, ACS Catal. 6 (2016) 6511–6519.
[18] K. Chen, Z. Chai, C. Li, L. Shi, M. Liu, Q. Xie, Y. Zhang, D. Xu, A. Manivannan, Z. Liu, ACS Nano 10 (2016) 3665–3673.
[19] Q. Liu, T. Chen, Y. Guo, Z. Zhang, X. Fang, Appl. Catal. B Environ. 205 (2017) 173–181.
[20] B. Lin, H. An, X. Yan, T. Zhang, J. Wei, G. Dong, Appl. Catal. B Environ. 210 (2017) 173–183.
[21] Y. Deng, L. Tang, G. Zeng, Z. Zhu, M. Yan, Y. Zhou, J. Wang, Y. Liu, J. Wang, Appl. Catal. B Environ. 203 (2017) 343–354.
[22] X. She, L. Liu, H. Ji, Z. Mo, Y. Li, L. Huang, D. Du, H. Xu, H. Li, Appl. Catal. B Environ. 187 (2016) 144–153.
[23] G. Liu, P. Niu, C. Sun, S.C. Smith, Z. Chen, G. Qing, H. Cheng, J. Am. Chem. Soc. 132 (2010) 11642–11648.
[24] Y. Zhu, T. Ren, Z. Yuan, ACS Appl. Mater. Interfaces 7 (2015) 16850–16856.
[25] J. Liu, H. Xu, Y. Xu, Y. Song, J. Lian, Y. Zhao, L. Wang, L. Huang, H. Ji, H. Li, Appl. Catal. B Environ. 207 (2017) 429–437.
[26] X. Yang, Z. Chen, J. Xu, H. Tang, K. Chen, Y. Jiang, ACS Appl. Mater. Interfaces 7 (2015) 15285–15293.
[27] Y. Hong, Y. Jiang, C. Li, W. Fan, X. Yan, M. Yan, W. Shi, Appl . Catal. B Environ. 180 (2016) 663–673.
[28] M. Xie, Y. Feng, X. Fu, P. Luan, L. Jing, J. Alloys Compd. 631 (2015) 120–124.
[29] J. Wu, H. Lu, X. Zhang, F. Raziq, Y. Qu, L. Jing, Chem. Comm. 52 (2016) 5027–5029.
[30] S. Chen, R. Yan, X. Zhang, K. Hu, Z. Li, M. Humayun, Y. Qu, L. Jing, Appl. Catal. B Environ. 209 (2017) 320–328.
[31] C. Zhang, M. Zhou, G. Ren, X. Yu, L. Ma, J. Yang, F. Yu, Water Res. 70 (2015) 414–424.
[32] M. Humayun, A. Zada, Z. Li, M. Xie, X. Zhang, Y. Qu, F. Raziq, L. Jing, Appl. Catal. B Environ. 180 (2016) 219–226.
[33] S. Yan, Z. Li, Z. Zou, Langmuir 25 (17) (2009) 10397–10401.
[34] J. Xu, L. Zhang, R. Shi, Y. Zhu, J. Mater. Chem. A 1 (2013) 14766–14772.
[35] J. Mao, T. Peng, X. Zhang, K. Li, L. Ye, L. Zan, Catal. Sci. Technol. 3 (2013) 1253–1260.
[36] F. Wang, P. Chen, Y. Feng, Z. Xie, Y. Liu, Y. Su, Q. Zhang, Y. Wang, K. Yao, W. Lv, G. Liu, Appl. Catal. B Environ. 207 (2017) 103–113.
[37] H. Xu, L. Zhang, J. Phys.Chem. C 114 (2010) 11534–11541.
[38] J. Murcia, M. Hidalgo, J. Navío, J. Araña, J.M. Dona-Rodríguez, Appl. Catal. B Environ. 179 (2015) 305–312.
[39] H. Huang, X. Li, X. Han, N. Tian, Y. Zhang, T. Zhang, Phys. Chem. Chem. Phys. 17 (2015) 3673–3679.
[40] F. Liang, Y. Zhu, Appl. Catal. B Environ. 180 (2016) 324–329.